Measuring Crowd Collectiveness

Bolei Zhou[1], Xiaoou Tang[1,3], and Xiaogang Wang[2,3]
[1]Department of Information Engineering, The Chinese University of Hong Kong
[2]Department of Electronic Engineering, The Chinese University of Hong Kong
[3]Shenzhen Institutes of Advanced Technology, Chinese Academy of Sciences
zhoubolei@gmail.com, xtang@ie.cuhk.edu.hk, xgwang@ee.cuhk.edu.hk

Abstract

Collective motions are common in crowd systems and have attracted a great deal of attention in a variety of multidisciplinary fields. Collectiveness, which indicates the degree of individuals acting as a union in collective motion, is a fundamental and universal measurement for various crowd systems. By integrating path similarities among crowds on collective manifold, this paper proposes a descriptor of collectiveness and an efficient computation for the crowd and its constituent individuals. The algorithm of the Collective Merging is then proposed to detect collective motions from random motions. We validate the effectiveness and robustness of the proposed collectiveness descriptor on the system of self-driven particles. We then compare the collectiveness descriptor to human perception for collective motion and show high consistency. Our experiments regarding the detection of collective motions and the measurement of collectiveness in videos of pedestrian crowds and bacteria colony demonstrate a wide range of applications of the collectiveness descriptor[1].

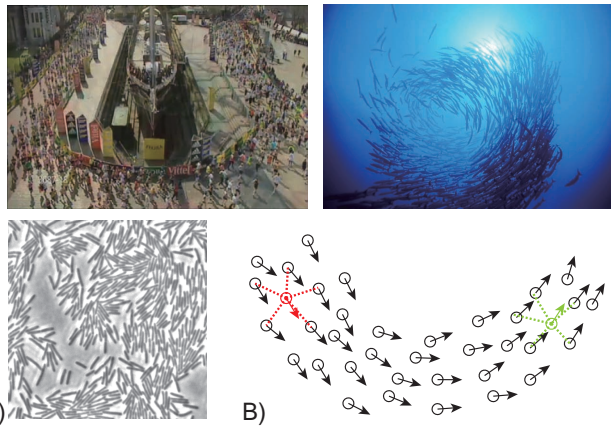

Figure 1. A) Collective motions of human crowd, fish shoal, and bacterial colony. B) Spatially coherent structures, *i.e.*, *Collective Manifold*, emerging in these crowds. Since individuals in a crowd system only coordinate their behaviors in their neighborhood, individuals at a distance may have low velocity correlation even though they are on the same collective manifold. An example of this is the red individual and the green individual. Thus, accurately measuring the collectiveness of crowd and its constituent individuals is challenging. Colored dash links represent neighborhoods.

1. Introduction

One of the most captivating phenomena in nature is the collective motion of crowds. From bacterial colonies and insect swarms to fish shoal, collective motions widely exist in different crowd systems and reflect the ordered macroscopic behaviors of constituent individuals. Many interdisciplinary efforts have been made to explore the underlying principles of this phenomenon. Physicists treat crowds as sets of particles and use equations from fluid mechanics to characterize individual movements and their interactions [9]. Behavioral studies show that complex crowd behaviors may result from repeated simple interactions among its constituent individuals, *i.e.*, individuals locally coordinate their behaviors with their neighbors then the crowd is self-organized into collective motion without external control [15, 17]. Meanwhile, animal aggregation is considered as an evolutionary advantage for species survival, since the integrated whole of individuals can generate complex patterns, quickly process information, and engage in collective decision-making [6].

One remarkable observation of collective motions in different crowd systems is that some spatially coherent structures often emerge from the movements of crowd, such as the arch-like macro structures in the human crowd, the fish shoal and the bacterial colony shown in Fig.1. We refer to the spatially coherent structure of collective motion as *Collective Manifold*. Fig.1 illustrates one important structural property of collective manifold: behavior consistency remains high among individuals in local neighborhood, but

[1]Data and codes are available at http://mmlab.ie.cuhk.edu.hk/project/collectiveness/

low among those that are far apart, even on the same collective manifold. In fact, individuals in crowds only have limited local sensing range, and often base their movements on locally acquired information such as the positions and motions of their neighbors. Some empirical studies have explored the importance of topological relations and information transmission among neighboring individuals in crowd [2]. However, there is a lack of quantitative analysis of this structural property of crowds.

Collectiveness describes the degree of individuals acting as a union in collective motion. It depends on multiple factors, such as the decision making of individuals and crowd density. Quantitatively measuring this universal property and comparing it across different crowd systems are important in order to understand the general principles of various crowd behaviors. Furthermore, this measurement plays important roles in many applications, such as monitoring the transition of a crowd system from disordered to ordered states, studying the correlation between collectiveness and crowd properties such as population density, characterizing the dynamic evolution of collective motion, and comparing the collectiveness of different crowd systems. Most existing crowd surveillance technologies [12, 27] cannot compare crowd behaviors across different scenes because they lack universal descriptors with which to characterize crowd dynamics. Monitoring collectiveness is also useful in crowd management, control of swarming desert locusts [5], prevention of disease spreading [22], and many other fields. However, this important property lacks accurate measurements. Existing works [3, 19] simply measured the average velocity of all the individuals to indicate the collectiveness of the whole crowd, which is neither accurate nor robust. The collectiveness of individuals in crowd is also ill-defined.

In this paper, by quantifying the topological properties of collective manifold of crowds, we propose a descriptor of collectiveness for crowd systems as well as their constituent individuals. Based on collectiveness, an algorithm called Collective Merging is proposed to detect collective motions from random motions. We validate the effectiveness and robustness of the proposed collectiveness on self-driven particles [19]. It is further compared to human motion perception for collective motion on a new video dataset with ground-truth. In addition, our experiments of detecting collective motions and measuring crowd collectiveness in videos of pedestrian crowds and bacterial colony demonstrate the wide applications of the collectiveness descriptor.

1.1. Related Works

Scientific studies on collective motion in crowd systems can be categorized as empirical or theoretical; a compact review can be found in [20]. In the computer vision community, crowd motion analysis has become an active research topic in recent years. Many approaches have focused on segmenting the motion patterns and learning the pedestrian behaviors. For example, Rabaud *et al.* [16] and Zhou *et al.* [25] detected independent/collective motions for object counting and clustering. Lin *et al.* [12] and Ali *et al.* [1] segmented motion fields generated by crowds. Zhou *et al.* [27] used a mixture of dynamic systems to learn pedestrian dynamics and applied it to crowd simulation. There are other works of crowd behavior analysis on surveillance applications, such as abnormal activity detection [13, 11] and semantic region analysis [26, 21]. Kratz *et al.* [10] proposed *efficiency* to measure the difference between the actual motion and intended motion of pedestrians for tracking and abnormality detection. However, none of the above-mentioned measured the collectiveness of crowd behaviors or explored its potential applications.

$\lvert \cdot \rvert$	Cardinality of a set.
$[.]_i$	i-th element of a vector.
$\mathbf{e}$	vector with all elements as 1.
$\mathbf{W}^n$	n power of a matrix $\mathbf{W}$.
$\max(x, y)$	maximum value of x and y.

Table 1. Notations used in the paper.

2. Measuring Collectiveness

A crowd is more than a gathering of individuals. Under certain circumstances, individuals in a crowd are organized into a unity with different levels of collective motions. Thus, crowd collectiveness should be determined by the collectiveness of its constituent individuals, which reflects the similarity of the individual's behavior to others in the same crowd system. We introduce collectiveness in a bottom-up manner: from behavior consistency in neighborhoods of individuals to that among all pairwise individuals, then from individual collectiveness to crowd collectiveness.

2.1. Behavior Consistency in Neighborhood

We first measure the similarity of individual behaviors in neighborhood. When individual j is in the neighborhood of i, *i.e.*, $j \in \mathcal{N}(i)$ at time t, the similarity is defined as

$$w_t(i, j) = \max(C_t(i, j), 0), \tag{1}$$

where $C_t(i, j)$ is the velocity correlation at t between i and j. $\mathcal{N}$ is defined as K-nearest-neighbor, motivated by existing empirical studies of collective motion, which have shown that animals maintain local interaction among neighbors with a fixed number of neighbors on topological distance, rather than with all neighbors within a fixed spatial distance [2]. Thus, $w_t(i, j) \in [0, 1]$ measures an individual's behavior consistency in a neighborhood. This pairwise similarity would be unreliable if two individuals are not neighbors because of the property of collective manifold

illustrated in Fig.1B. A better behavior consistency based on the structural property of collective manifold is proposed below.

2.2. Behavior Consistency on Collective Manifold

Since similarity cannot be accurately estimated when two individuals are at a distance, we propose a new pairwise similarity based on an important topological structure of collective manifold: paths, which represent the connectivity of the network associated with a graph [4]. In crowd systems, paths have important roles in information transmission and communication among constituent individuals. Thus, path-based similarity can better characterize the behavior consistency among individuals in a crowd.

Let $\mathbf{W}$ be the weighted adjacency matrix of the graph associated with a crowd set $\mathcal{C}$, where an edge $w_t(i,j)$ is the similarity between individual i and j in its neighborhood defined in Eq.1. Let $\gamma_l = \{p_0 \rightarrow p_1 \rightarrow ... \rightarrow p_l\}$ $(p_0 = i, p_l = j)$ denote a path of length l through nodes $p_0, p_1, ..., p_l$ on $\mathbf{W}$ between individual i and j. Then $\nu_{\gamma_l} = \prod_{k=0}^{l} w_t(p_k, p_{k+1})$ is defined as the *path similarity* on a *specific* path γ_l.

Since there can be more than one path of length l between i and j, let the set $\mathcal{P}_l$ contain all the paths of length l between i and j; then the l-path similarity is defined as

$$\nu_l(i,j) = \sum_{\gamma_l \in \mathcal{P}_l} \nu_{\gamma_l}(i,j). \tag{2}$$

$\nu_l(i,j)$ can be efficiently computed with Theorem 1.

Theorem 1. *$\nu_l(i,j)$ is the (i,j) entry of matrix $\mathbf{W}^l$.*

2.3. Individual Collectiveness from Path Similarity

Since l-path similarity $\nu_l(i,j)$ measures the behavior consistency between i and j at l-path scale, we define the individual collectiveness of individual i at l-path scale as

$$\phi_l(i) = \sum_{j \in \mathcal{C}} \nu_l(i,j) = [\mathbf{W}^l \mathbf{e}]_i. \tag{3}$$

Fig.2B plots the average ϕ_l (in log scale) with $l = 1 \sim 30$ in a synthetic collective crowd shown in Fig.2A. The value of average ϕ_l exponentially increases with l, because the number of paths between two nodes in a well connected graph increases exponentially with the path length.

To further measure crowd collectiveness, we should integrate the individual collectiveness at all path scales; that is, $\{\phi_1, ..., \phi_l, ..., \phi_\infty\}$. However, due to the exponential increase of ϕ_l with l shown in Fig.2B, individual collectiveness at different path scales cannot be directly summed. Therefore, we define a generating function to integrate all path similarities.

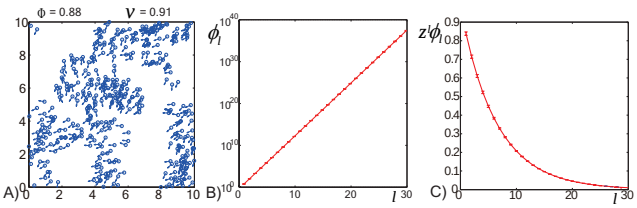

Figure 2. A) Synthetic crowd from Self-Driven Particles in collective motion (details of SDP are given in Section 3). B) Plot of average ϕ_l (in log scale) with l. C) Regularization of path similarity. Individual collectiveness at lower l-path scales make a greater contribution to the overall individual collectiveness.

2.4. Crowd Collectiveness with Regularization

Generating function regularization is used to assign a meaningful value for the sum of a possibly divergent series [7]. There are different forms of generating functions. We define the generating function for the l-path similarities as

$$\varpi_{i,j} = \sum_{l=1}^{\infty} z^l \nu_l(i,j), \tag{4}$$

where z is a real-valued regularization factor, and z^l can be interpreted as the weight for l-path similarity. $z < 1$ and cancels the effect that ϕ_l exponentially increases with l. $\varpi_{i,j}$ can be computed with Theorem 2.

Theorem 2. *$\varpi_{i,j}$ is the (i, j) entry of matrix $\mathbf{Z}$, where $\mathbf{Z} = (\mathbf{I} - z\mathbf{W})^{-1} - \mathbf{I}$ and $0 < z < \frac{1}{\rho(\mathbf{W})}$. $\rho(\mathbf{W})$ denotes the spectral radius of matrix $\mathbf{W}$.*

Individual collectiveness from the generating function regularization on all the path similarities can be written as

$$\phi(i) = \sum_{l=1}^{\infty} z^l \phi_l(i) = [\mathbf{Z}\mathbf{e}]_i. \tag{5}$$

In Fig.2C, we let $z = \frac{0.9}{\rho(\mathbf{W})}$ and plot the average $z^l\phi_l$ which approaches 0 as l increases. The summation of regularized individual collectiveness from all path scales converges. z controls the convergence rate and the relative contributions of path similarities with different lengths to ϕ.

The crowd collectiveness of a crowd system $\mathcal{C}$ is then defined as the mean of all the individual collectiveness, which can be explicitly written in a closed form as

$$\Phi = \frac{1}{|\mathcal{C}|} \sum_{i=1}^{|\mathcal{C}|} \phi(i) = \frac{1}{|\mathcal{C}|} \mathbf{e}^\top ((\mathbf{I} - z\mathbf{W})^{-1} - \mathbf{I})\mathbf{e}. \tag{6}$$

Φ captures the structural property of the whole dataset. Such structure-based descriptors are also effectively used in general data clustering [24, 23].

3. Properties of the Collectiveness

We derive some important properties of collectiveness.

Algorithm 1 Collective Merging

INPUT: $\{\mathbf{x}_i, \mathbf{v}_i | i \in \mathcal{C}\}_t$.

1:Compute $\mathbf{W}$ from K-NN using Eq. 1.

2:$\mathbf{Z} = (\mathbf{I} - z\mathbf{W})^{-1} - \mathbf{I}$.

3:Set the entry $\mathbf{Z}(i,j)$ to 1 if $\mathbf{Z}(i,j) \geq \kappa$, otherwise to 0.

4:Extract the connected components of the thresholded $\mathbf{Z}$.

Property 1. (Strong Convergence Condition) $\mathbf{Z}$ *converges when* $z < \frac{1}{K}$.

It is computationally expensive to choose z by comparing it with $\rho(\mathbf{W})$, especially for a large crowd system, since we need to compute the eigenvalues of $\mathbf{W}$ to get $\rho(\mathbf{W})$ with complexity $\mathcal{O}(n^3)$. According to Property 1, the value of z can be determined without computing $\rho(\mathbf{W})$.

Property 2. (Bounds of Φ) $0 \leq \Phi \leq \frac{zK}{1-zK}$, *if* $z < \frac{1}{K}$.

The equality stands when $\mathbf{W} = \mathbf{A}$, where $\mathbf{A}$ is the $1-0$ adjacency matrix from K-nearest-neighbor. $\mathbf{W} = \mathbf{A}$ indicates that there are perfect velocity correlations among neighbors; that is, $w_t(i,j) = 1$ if $j \in \mathcal{N}(i)$ for any i, which means that all the constituent individuals in neighborhood move in the same direction. For simplicity, in most of our experiments we let $K = 20$ and $z = 0.025$, so the upper bound of Φ is 1. Relations among Φ, K and z are briefly discussed in Section 5.3.

Property 3. (Upper bound of entries of Z) $\varpi_{i,j} < \frac{z}{1-zK}$, *for every entry (i,j) of* $\mathbf{Z}$.

This property will be used in the following algorithm for detecting collective motion patterns from clutters.

4. Collective Motion Detection

Based on the collectiveness descriptor, we propose an algorithm called Collective Merging to detect collective motions from time-series data with noises (see Algorithm 1). Given spatial locations $\mathbf{x}_i$ and velocities $\mathbf{v}_i$ of individuals $i \in \mathcal{C}$ at time t, we first compute $\mathbf{W}$. By thresholding the values on $\mathbf{Z}$, we can easily remove outlier particles with low collectiveness and get the clusters of collective motion patterns as the connected components from thresholded $\mathbf{Z}$. As for the threshold κ, according to the bound in Property 3 we let $\kappa = \frac{\alpha z}{1-zK}$ where $0.4 < \alpha < 0.8$. Based on the accurate measurement of collectiveness, this four-lined algorithm can be implemented in real time. It has potential applications in time-series clustering and activity analysis. In the experiment section, we demonstrate its effectiveness for detecting collective motions in various videos.

5. Evaluation on Self-Driven Particles

We take the Self-Driven Particle model (SDP) [19] to evaluate the proposed collectiveness, because SDP has been used extensively for studying collective motion and shows high similarity with various crowd systems in nature [5, 22]. Importantly, the groundtruth of collectiveness in SDP is known for evaluation. SDP was firstly proposed to investigate the emergence of collective motion in a system of particles. These simple particles are driven with a constant speed, and the directions of their velocities are updated to the average direction of the particles in their neighborhood at each frame. It is shown that the level of random perturbation η on the aligned direction in neighborhood would cause the phase transition of this crowd system from disordered movements into collective motion. The update of velocity direction θ for every individual i in SDP is

$$\theta_i(t+1) = \langle \theta_j(t) \rangle_{j \in \mathcal{N}(i)} + \Delta\theta, \tag{7}$$

where $\langle \theta_j \rangle_{j \in \mathcal{N}(i)}$ denotes the average direction of velocities of particles within the neighborhood of i, $\Delta\theta$ is a random angle chosen with a uniform distribution within the interval $[-\eta\pi, \eta\pi]$. η tunes the level of alignment[2].

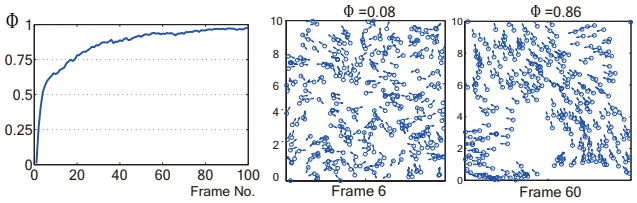

Figure 3. Emergence of collective motion in SDP. At the beginning, Φ is low since the spatial locations and moving directions of individuals are randomly assigned. The behaviors of individuals gradually turn into collective motion from random movements, and Φ accurately reflects the phase transition of crowd dynamics. Here $K = 20$, $z = 0.025$, and $\eta = 0$. The upper bound of Φ is 1.

5.1. Crowd Collectiveness of SDP

As shown in Fig.3, we compute crowd collectiveness Φ at each time t. Φ monitors the emergence of collective motion over time. At initialization, the spatial locations and velocity directions of all the particles are randomly assigned. The crowd gradually turns into the state of collective motion. Φ accurately records this phase transition.

As η increases, particles in SDP become disordered. As shown in Fig.4, Φ accurately measures the collectiveness of crowd systems under different levels of random perturbation η. For a comparison, Fig.4B plots the average normalized velocity $v = \| \frac{1}{N} \sum_{i=1}^{N} \frac{v_i}{\|v_i\|} \|$, which was commonly used as a measure of collectiveness in existing works [3, 19]. From the large standard deviation of v under multiple simulations with the same η, we see that v is unstable and sensitive to initialization conditions of SDP. On the contrary, Φ shows its robustness on measuring crowd collectiveness.

[2]In our implementation of SDP, the absolute value of velocity $\|v\|$=0.03, the number of individuals $N = 400$, and interaction radius $r = 1$. Experimental results in [19] have shown that these three parameters only have a marginal effect on the general behaviors of SDP.

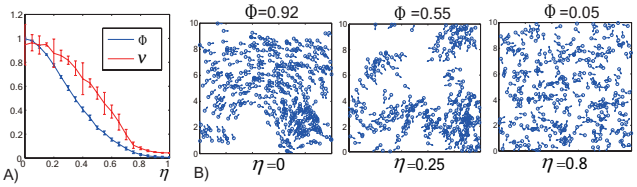

Figure 4. A) Φ and v with increasing η. The bars indicate the standard deviations of these two measurements. The large deviations of v show that v is unstable and sensitive to initialization of SDP. At each η, simulation repeats for 20 times. B) For a low η, all the individuals are in a global collective motion, and Φ is close to the upper bound. For a relatively larger η , individuals form multiple clusters of collective motions. For a high η, individuals move randomly and Φ is low.

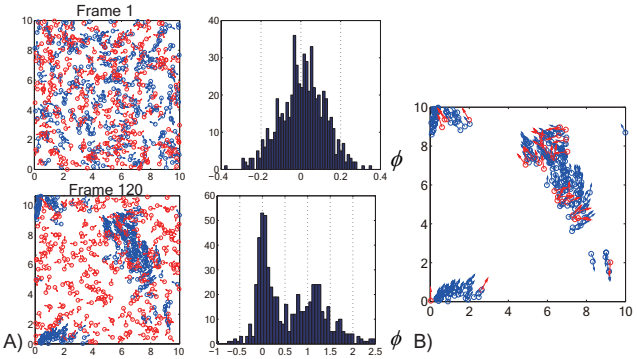

Figure 5. A) Two frames of the mixed-crowd system and their histograms of individual collectiveness. After a while, self-driven particles are organized into clusters of collective motions. The histogram of ϕ_t is clearly separated into two modes. B) By removing particles with individual collectiveness lower than 0.5, we can extract self-driven particles in collective motions. Blue and red points represent self-driven particles and outliers. The number of outliers is equal to that of self-driven particles and $\eta = 0$.

5.2. Collectiveness in Mixed-Crowd Systems

SDP assumes that all the individuals are homogeneous. Studies on complex systems [14] have shown that individuals in most crowd systems in nature are inhomogeneous. To evaluate the robustness of our collectiveness descriptor, we extend SDP to a mixed-crowd model by adding outlier particles, which do not have alignment in neighborhoods and move randomly all the time. We measure individual collectiveness in this mixed-crowd system. As shown in Fig.5A, individuals are randomly initialized at the start, so the histogram of individual collectiveness has a single mode. When self-driven particles gradually turn into clusters of collective motions, there is a clear separation between two modes in the histogram of individual collectiveness. By removing individuals with collectiveness smaller than 0.5, we can effectively extract collectively moving self-driven particles from outliers as shown in Fig.5B.

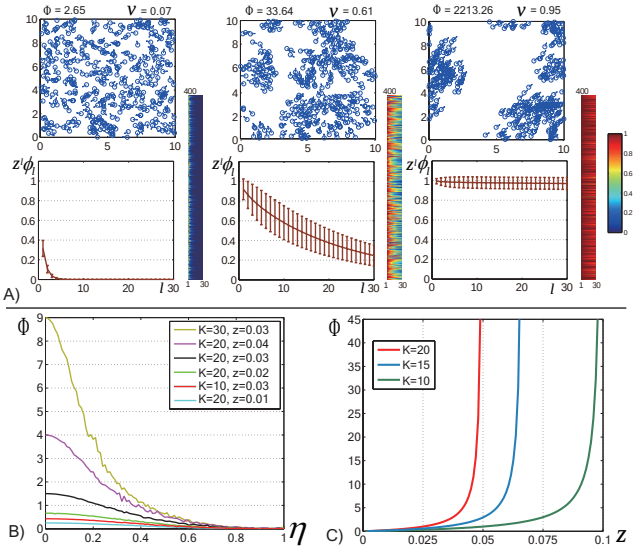

Figure 6. A) Regularized individual collectiveness on l-path scale $z^l\phi_l$ as $\eta = 0$ and $z = \frac{1}{K}$ at three different levels of collective motions. In each diagrams, the left-hand side shows the average $z^l\phi_l$ with $l = 1 \sim 30$ and the right-hand side shows the visualization of all the values of $z^l\phi_l(i)$ with $l = 1 \sim 30$ and $i = 1 \sim 400$. Since the convergence condition is not satisfied, Φ become unstable when SDP is in a high level of collective motion. B) Φ with increasing η at different K and z in SDP. C) Given a fixed K, the upper bound of Φ grows fast when z approaches to $\frac{1}{K}$, which makes Φ unstable.

5.3. Convergence Condition of Collectiveness

Property 1 shows that $\mathbf{Z}$ converges when $z < \frac{1}{K}$. What happens if $z \geq \frac{1}{K}$? We let $z = \frac{1}{K}$ and plot the regularized individual collectiveness of l-path scales $[z\phi_1, z^2\phi_2, ..., z^l\phi_l]$ in Fig.6. As the SDP gradually turns into collective motion, $z^l\phi_l$ with large l-path scale approaches to 1, which makes $\sum_{l=1}^{\infty} z^l\phi_l$ non-convergent, and crowd collectiveness Φ unstable.

There are two parameters z and K for computing collectiveness in practical applications. K defines the size of neighborhood and z makes the series summation converge. K affects similarity estimation in neighborhood. A large K makes the estimation inaccurate, while a small K is sensitive to noise. Empirically it could be 5%$\sim$10% of $|\mathcal{C}|$. In all our experiments, we fix $K = 20$. z is constrained by K in Property 1. With different K and z, the upper bound of Φ varies, as shown in Fig.6B. With a larger upper bound, the derivative $\frac{d\Phi}{d\eta}$ is larger and the measurement is more sensitive to the change of crowd motion. Φ can also be re-scaled to [0, 1] divided by the upper bound. Thus, by tuning z and K we can control the sensitivity of collectiveness in practical applications. The upper bound of Φ grows quickly when z approaches to $\frac{1}{K}$, which makes the value of Φ unstable, as shown in Fig.6C. The ideal range is $\frac{0.4}{K} < z < \frac{0.8}{K}$.

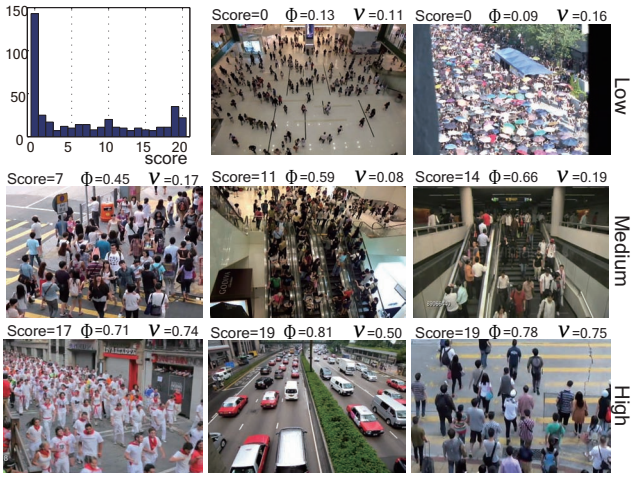

Figure 7. Histogram of collective scores of all the videos in the Collective Motion Database and some representative video frames, along with their collective scores, Φ, and v. The three rows are from the three collectiveness categories.

6. Further Evaluation and Applications

We evaluate the consistency between our collectiveness and human perception, and apply the proposed descriptor and algorithm to various videos of pedestrian crowds and bacterial colony.

6.1. Human Perception for Collective Motion

To quantitatively evaluate the proposed crowd collectiveness, we compare it with human motion perception on a new Collective Motion Database, and then analyze the consistency and correlation with human-labeled ground-truth for collective motion. The Collective Motion Database consists of 413 video clips from 62 crowded scenes. 116 clips are selected from Getty Image [8], 297 clips are captured or collected by us. This database contains different levels of collective motions with 100 frames per clips. Some representative frames are shown in Fig. 7. To get the ground-truth, 10 subjects are invited to rate all videos independently. A subject is asked to rate the level of collective motions in a video from three options: low, medium, and high. We propose two criteria to evaluate the consistency between human-labeled ground-truth and the proposed collectiveness descriptor.

The first is the correlation between the human scores and our collectiveness descriptor. We count the low option as 0, the medium one as 1, and the high one as 2. Since each video is labeled by ten subjects, we sum up all the scores as the collective score for this video. The range of collective scores is [0, 20]. The histogram of collective scores for the whole database is plotted in Fig.7. We compute the crowd collectiveness Φ at each frame using the motion features extracted with a generalized KLT (gKLT) tracker derived from [18], and take Φ averaged over 100 frames as the collectiveness for this video. We compute v using the same motion features as a comparison baseline. Fig.7 shows the collective scores, Φ, and v for some representative videos. Fig.8A scatters the collective scores with Φ and v of all the videos, respectively. There is a high correlation between collective scores and Φ, and the proposed collectiveness is consistent with human perception.

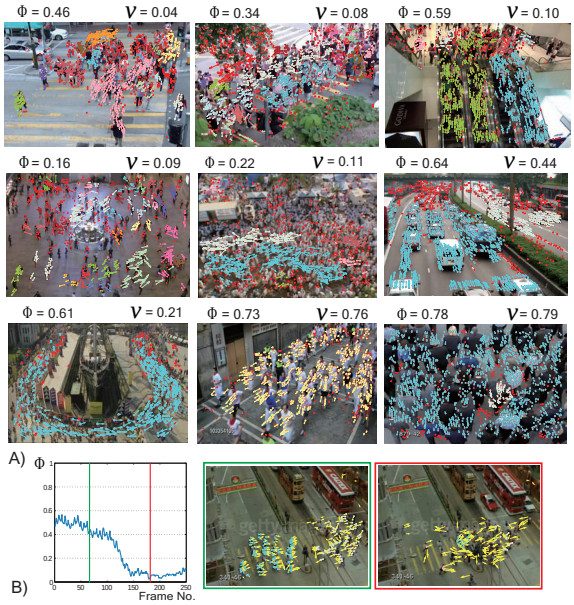

Figure 9. A) Detecting collective motions from crowd videos. Keypoints with the same color belong to the same cluster of collective motion. Red crosses are detected outliers. B) Monitoring crowd dynamics with collectiveness. Two frames indicate the representative states of the crowd.

The second is the classification accuracy based on the collectiveness descriptor. We divide all the videos into three categories by majority voting of subjects' rating, and then evaluate how the proposed collectiveness descriptor can classify them. Histograms of Φ and v for the three categories are plotted effectively in Fig.8B. Φ has better discrimination capability than v. Fig.8C plots the ROC curves and the best accuracies which can be achieved with all the possible decision boundaries for binary classification of high and low, high and medium, and medium and low categories based on Φ and v, respectively. Φ can better classify different levels of collective motions than v, especially on the binary classification of high-medium categories and medium-low categories of videos. It indicates our collectiveness descriptor can delicately measure the dynamic state of crowds.

Classification failures come from two sources. Since there are gray areas between high-medium and medium-low collective motions, some samples are even difficult for humans to reach consensus and are also difficult to our descriptor. Meanwhile collectiveness may not be properly computed due to tracking failures, projective distortion and

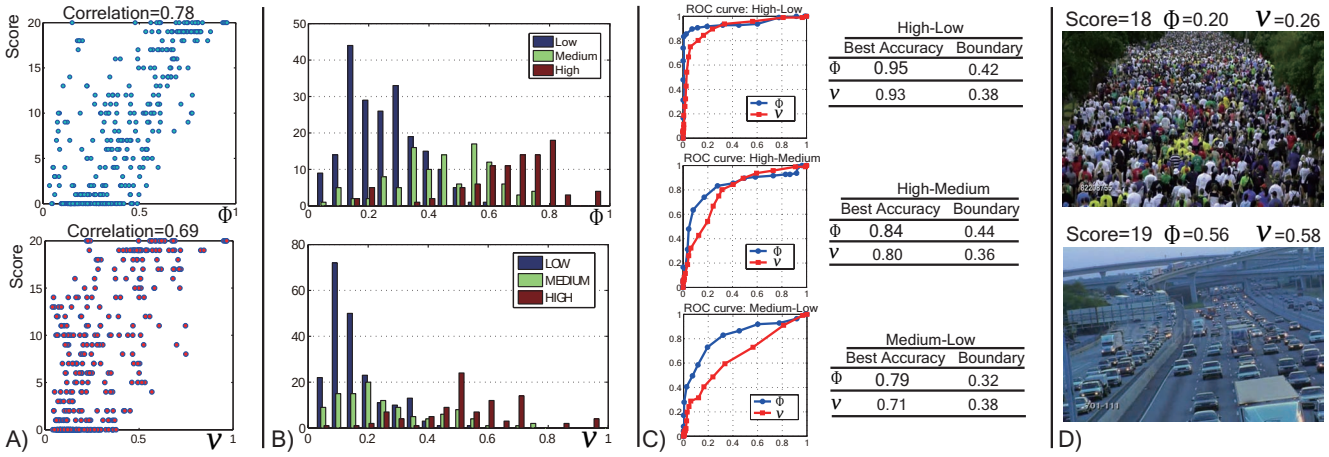

Figure 8. A) Scatters of collective scores with Φ and v for all the videos. B) Histograms of Φ and v for the three categories of videos. C) ROC curves and best accuracies for high-low, high-medium, and medium-low classification. D) Failure examples of collectiveness.

special scene structures. Two failure examples are shown in Fig.8D. The computed collectiveness in the two videos is low because the KLT tracker does not capture the motions well due to the perspective distortion and the extremely low frame rate, while all subjects give high scores because of the regular pedestrian and traffic flows in the scenes.

6.2. Collective Motion Detection in Videos

We detect collective motions from videos in the Collective Motion Database. Collective motion detection in crowd videos is challenging due to the short and fragmented nature of extracted trajectories, as well as the existence of outlier trajectories. Fig.9A shows the detected collective motions by Collective Merging on nine videos, along with their computed Φ and v. The detected collective motion patterns correspond to a variety of behaviors, such as group walking, lane formation, and different traffic modes, which are of a great interest for further video analysis and scene understanding. The estimated crowd collectiveness also varies across scenes and reflects different levels of collective motions in videos. However, v cannot accurately reflect the collectiveness of crowd motions in these videos.

Furthermore, the proposed crowd collectiveness can be used to monitor crowd dynamics. Fig.9B shows an example in which the collectiveness changes abruptly when two groups of pedestrians pass each other. Such events indicate rapid phase transition of a crowd system or some critical point has been reached. They are useful for crowd control and scientific studies.

6.3. Collective Motions in Bacterial Colony

In this experiment, we use the proposed collectiveness to study collective motions emerging in a bacterial colony. The wild-type *Bacillus subtilis* colony grows on agar substrates, and bacteria inside the colony freely swim on the agar surface. The real motion data of individual bacteria comes from [22]. There are $200 \sim 400$ bacteria moving around at every frame. Fig.10AB plot Φ and v with the number of bacteria over time. Fig.10C shows representative frames and collective motion patterns detected by Collective Merging. Crowd density was proved to be one of the key factors for the formation of collective motion [22, 19]. A lot of scientific studies are conducted to analyze their correlation. For the same type of bacteria in the same environment, bacteria collectiveness should monotonically increase with density. Fig.10A shows that bacteria density has a much better correlation with Φ than v. Our proposed collectiveness measurement has good potentials for scientific studies.

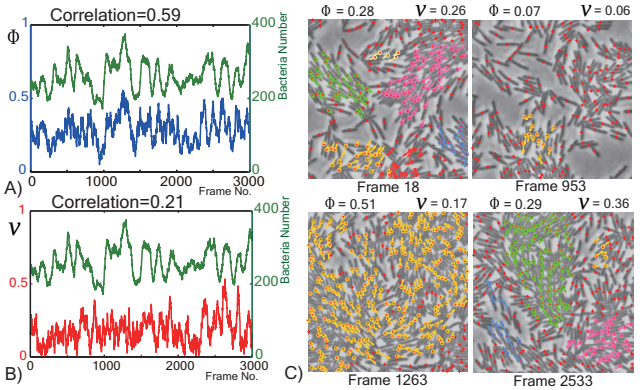

Figure 10. A) The crowd collectiveness of the bacterial colony and the bacteria number change over time; their correlation is high. B) The average normalized velocity of the bacterial colony and the bacteria number change over time; their correlation is low. C) Representative frames of collective motion patterns detected by Collective Merging and their Φ and v. Arrows with different colors indicate different clusters of detected collectively moving bacteria. Red crosses indicate detected randomly moving bacteria.

7. Conclusions and Future Work

We have proposed a collectiveness descriptor for crowd systems as well as their constituent individuals along with the efficient computation. Collective Merging can be used to detect collective motions from randomly moving outliers. We have validated the effectiveness and robustness of the proposed collectiveness on the system of self-driven particles, and shown the high consistency with human perception for collective motion. Further experiments on videos of pedestrian crowds and bacteria colony demonstrate its potential applications in video surveillance and scientific studies.

As a new universal descriptor for various types of crowd systems, the proposed crowd collectiveness should inspire many interesting applications and extensions in future work. Individuals in a crowd system can move collectively in a single group or in several groups with different collective patterns, even though the system has the same value of Φ. Our single collectiveness measurement can be well extended to a spectrum vector of characterizing collectiveness at different length scales. It is also desirable to enhance the descriptive power of collectiveness by modeling its spatial and temporal variations. The enhanced descriptor can be applied to cross-scene crowd video retrieval, which is difficult previously because universal properties of crowd systems could not be well quantitatively measured. Collectiveness also provides useful information in crowd saliency detection and abnormality detection. This paper is an important starting point in these exciting research directions.

Acknowledgment

This work is partially supported by the General Research Fund sponsored by the Research Grants Council of Hong Kong (Project No. CUHK417110 and CUHK417011) and National Natural Science Foundation of China (Project No.61005057 and 2192019). The first author would like to thank Deli Zhao and Wei Zhang for valuable discussions and Hepeng Zhang for sharing bacteria data.

References

[1] S. Ali and M. Shah. Floor fields for tracking in high density crowd scenes. In *Proc. ECCV*, 2008.

[2] M. Ballerini, N. Cabibbo, R. Candelier, A. Cavagna, E. Cisbani, I. Giardina, V. Lecomte, A. Orlandi, G. Parisi, A. Procaccini, et al. Interaction ruling animal collective behavior depends on topological rather than metric distance: Evidence from a field study. *Proceedings of the National Academy of Sciences*, 2008.

[3] M. Ballerini, N. Cabibbo, et al. Empirical investigation of starling flocks: a benchmark study in collective animal behaviour. *Animal behaviour*, 2008.

[4] N. Biggs. *Algebraic graph theory*. Cambridge Univ Pr, 1993.

[5] J. Buhl, D. Sumpter, I. Couzin, J. Hale, E. Despland, E. Miller, and S. Simpson. From disorder to order in marching locusts. *Science*, 312:1402–1406, 2006.

[6] I. Couzin. Collective cognition in animal groups. *Trends in Cognitive Sciences*, 2009.

[7] E. Elizalde. *Ten physical applications of spectral zeta functions*. Springer Verlag, 1995.

[8] GettyImage. http://www.gettyimages.com/.

[9] R. Hughes. The flow of human crowds. *Annual Review of Fluid Mechanics*, 2003.

[10] L. Kratz and K. Nishino. Going with the flow: Pedestrian efficiency in crowded scenes. In *Proc. ECCV*, 2012.

[11] L. Kratz and K. Nishino. Tracking pedestrians using local spatio-temporal motion patterns in extremely crowded scenes. In *IEEE Trans. on PAMI*, 2012.

[12] D. Lin, E. Grimson, and J. Fisher. Learning visual flows: A lie algebraic approach. In *Proc. CVPR*, 2009.

[13] V. Mahadevan, W. Li, V. Bhalodia, and N. Vasconcelos. Anomaly detection in crowded scenes. In *Proc. CVPR*, 2010.

[14] J. Miller and S. Page. *Complex adaptive systems: An introduction to computational models of social life*. Princeton Univ Pr, 2007.

[15] M. Moussaid, S. Garnier, G. Theraulaz, and D. Helbing. Collective information processing and pattern formation in swarms, flocks, and crowds. *Topics in Cognitive Science*, 2009.

[16] V. Rabaud and S. Belongie. Counting crowded moving objects. In *Proc. CVPR*, 2006.

[17] C. Reynolds. Flocks, herds and schools: A distributed behavioral model. In *ACM SIGGRAPH Computer Graphics*, 1987.

[18] C. Tomasi and T. Kanade. Detection and Tracking of Point Features. In *Int'l Journal of Computer Vision*, 1991.

[19] T. Vicsek, A. Czirók, E. Ben-Jacob, I. Cohen, and O. Shochet. Novel type of phase transition in a system of self-driven particles. *Physical Review Letters*, 1995.

[20] Z. A. Vicsek T. Collective motion. *arXiv:1010.5017*, 2010.

[21] X. Wang, X. Ma, and W. Grimson. Unsupervised activity perception in crowded and complicated scenes using hierarchical bayesian models. *IEEE Trans. on PAMI*, 2008.

[22] H. Zhang, A. Ber, E. Florin, and H. Swinney. Collective motion and density fluctuations in bacterial colonies. *Proceedings of the National Academy of Sciences*, 2010.

[23] W. Zhang, D. Zhao, and X. Wang. Agglomerative clustering via maximum incremental path integral. *Pattern Recognition*, 2013.

[24] D. Zhao and X. Tang. Cyclizing clusters via zeta function of a graph. In *In Advances in Neural Information Processing Systems*, 2008.

[25] B. Zhou, X. Tang, and X. Wang. Detecting coherent motions from crowd clutters. In *Proc. ECCV*, 2012.

[26] B. Zhou, X. Wang, and X. Tang. Random field topic model for semantic region analysis in crowded scenes from tracklets. In *Proc. CVPR*, 2011.

[27] B. Zhou, X. Wang, and X. Tang. Understanding collective crowd behaviors: Learning a mixture model of dynamic pedestrian-agents. In *Proc. CVPR*, 2012.